Curvature Based Shape Estimation Using Tactile Sensing

M. Charlebois, K. Gupta[*]**, and S. Payandeh**[*]
Experimental Robotics Lab (ERL), Simon Fraser University
School of Engineering Science, Burnaby, B.C. V5A LS6, Canada

Abstract

In this paper we propose an approach - we call it a "Blind Man's" approach - to shape description in which tactile information is sensed from the fingertips of a dexterous hand. Using this contact information, we investigate two complementary methods for curvature estimation. The first method is based on rolling one finger to estimate curvature at a point on the surface. We use Montana's equations for estimating curvature at a point using simulations and analyze the sensitivity of the approach to noise. The second method uses multiple fingers to slide along a surface while sensing contact points and surface normals. We present a method to extract the shape properties of a patch obtained by fitting a B-spline surface to this multi-fingered sweep across the surface of the object. The method enables us to extract higher level shape information based on the curvature properties of patch.

1 Introduction

Unlike vision, haptic sensing can extract information about many attributes of an object: shape, mass, volume, rigidity, texture, and temperature to name a few. When the hands manipulate an object they often occlude it from view. This would be a problem if vision was the only sensing modality.

We adopt a "Blind Man's" approach in which tactile information from the tips of the fingers is the only sensing modality. This enables us to sense the contact point, and surface normal because the geometry of the probe and the configuration parameters of the manipulator are known.

Human's sense of touch is rich in the amount of information it can acquire simultaneously. However, humans use specialized Exploratory Procedures (EPs) to extract specific information about an object as described by Klatzky and Lederman [8]. Their investigations also found that shape was the most highly diagnostic property for recognition. They describe a Contour Following EP which humans use to determine the exact and local shape properties of an object.

We investigate two EPs for shape perception using fingertip tactile sensors: one based on rolling and the other based on gliding on the surface of the unknown object. Both of these EPs were discussed by Hemami, Bay, and Goddard in [7], however their focus was on the sensory requirements for performing these two EPs. Our methodology for obtaining more global shape information has been motivated by researchers in computer vision [4], [5], [10], [12],

[13] who have investigated aspects of shape description and modelling based on curvature properties.

Using these two EPs, local and more global shape properties of the object can be explored. Global data refers to the shape properties which are common to a surface patch or to regions of the patch. We assume that a dexterous robot hand with semi-spherical fingertip tactile sensors is used to probe an object. The curvature at a point on the surface can be estimated from rolling a finger tip on the surface of the object. More global shape properties a patch on a surface can be obtained by sweeping multiple fingers of the dexterous hand across the surface, fitting a patch to the locus of contact points, and then analyzing the curvature properties of the patch. The information gathered about the shape of the object could be used to orient the patch, guide further exploratory actions, or be used toward autonomous shape description or object recognition.

The scope of this paper is twofold: to investigate the feasibility of Montana's [9] approach for estimating local curvature using EP1, and to propose a method using EP2 to determine higher level shape properties.

Montana's presentation of estimating curvature from rolling did not include in its scope, a performance analysis of his method. In this paper we investigate the sensitivity of the approach to resolution and measurement error.

Allen and Michelman [1] have investigated the usage of EPs to find global shape and recognize surfaces of revolution from their contours. In this research, we are investigating a way to analyze more general curved surfaces and extract higher level shape information. Fearing [6] has also investigated recovering shape from extremely sparse tactile data. He attempted to recover a much restricted class of shape models from convex Linear Straight Homogeneous Generalized Cylinders (LSHGC) from three finger contacts. Using the position, surface normal, and curvature information at the contacts, Fearing attempted to solve the constraint equations of the LSHGC.

Unlike range images, tactile data is generally sparse and noisy. Curvature estimates at the contact points cannot be readily obtained based on the difference of adjacent points. We propose using multiple fingers to track a surface and then fitting a smoothing spline [3] to it. The contact normal information is also incorporated to assist in the approximation of the shape of the surface.

The structure of the paper is as follows. Section 2 provides an overview of the two EPs described earlier. In section 3 the equations used to estimate the local curvature and the

curvature at points on the B-spline surface are presented. Section 4 describes the simulation studies for curvature estimation from rolling and curvature based shape description of the B-spline surfaces. Conclusions are provided in Section 5.

2 Overview of EP1 and EP2

The rolling EP (EP1), and surface tracking EP (EP2) form the basis for curvature based shape estimation of an object using tactile sensing. EP1 estimates local curvature at a point on the surface, and EP2 explores a region of the surface whose shape can then be analyzed from its curvature properties. The following section describes these two EPs in greater detail.

2.1 Estimating Local Curvature (EP1)

The surface curvature at a point can be estimated from small rolling motions (we call them probes) in the neighborhood of the contact point. Montana derived the kinematics for two rigid bodies in rolling contact and described a method to determine the surface curvature at a point. We have verified this approach in simulation and analyzed its sensitivity to measurement error and sensor resolution.

Using this approach, it is required to rotate at a known angular velocity around a fixed axis in the instantaneous contact frame. The contact frame will be determined by the point of contact, the surface normal, and the initial contact configuration. The surface normal can be inferred from the point of contact when the geometry of the probe is known. The accuracy of the calculation of the contact frame will be determined by the resolution of the tactile sensor, the robot joint encoders and the calibration of the robot.
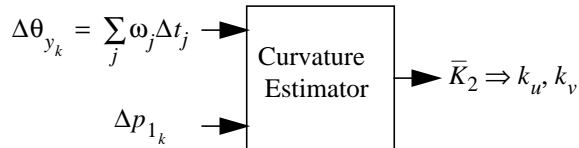
$$\Delta\theta_{y_k} = \sum_j \omega_j \Delta t_j \rightarrow \boxed{\begin{array}{c}\text{Curvature}\\\text{Estimator}\end{array}} \rightarrow \bar{K}_2 \Rightarrow k_u, k_v$$
$$\Delta p_{1_k} \rightarrow$$

Fig. 1. Input and Output of Curvature Estimator

The surface is parameterized by u and v based on its gauss map. The curvature at a point on the surface is estimated from eight probes: two in each of the u, $-u$, v, and $-v$ directions. $\Delta\theta_x$ and $\Delta\theta_y$ are the approximations of the sums of the instantaneous rotations about the x-axis and y-axis of the instantaneous contact frames for a particular probe. Δp_1 is the change of the contact point on the surface of the probe. The eight samples of $\Delta\theta_x$, $\Delta\theta_y$, and Δp_1 are used to determine the minimum error solution of the curvature form. The equation governing the evolution of the point of contact requires the angular velocity (ω) to be known. This equation is presented in section 3.1. Figure 1 shows the inputs and outputs of the curvature estimation procedure.

The returned values k_u and k_v are the normal curvatures in the u and v directions.

We define Δs as the length of the curve traced on the surface of the probe for a particular rolling motion. The evolution of the contact point on the probe as it rolls on the surface of the object is used to determine the curvature in the direction of motion. Probes in two independent directions are sufficient to determine the curvature although if more probes are performed a least squares fit can be calculated for greater confidence. This approach was tested in simulation and was able to recover the correct curvature form of the object being probed.

The normal curvature in a particular tangent direction is the reciprocal of the radius of curvature in that direction.

We define the relative curvature ratio (RCR) as the normal curvature of the object at the point of contact in a particular tangent direction divided by the normal curvature of the probe.

2.2 Estimating Shape Over a Region (EP2)

Sweeping multifinger probes are used to extract patches from the surface of the object in order to approximate a large portion of the surface using a small number of data points. A B-spline surface can be fit to the locus of points and the shape properties of the patch can be determined. A B-spline surface was chosen for its compact representation and because the B-spline representation of the scalar fields of the derivatives is known once the knots for the approximating surface have been calculated. This enables the Gaussian and mean curvatures to be easily calculated at a given point on the fitted surface.

In order to hypothesize the shape of the probed patch, the surface curvature must be determined. The shape of the patch is invariant to scale and orientation. Shape properties will be determined from the estimated Gaussian and mean curvatures over the patch. The signs of Gaussian and mean curvatures (Kg and Ka) yield a set of eight surface primitives. These primitives are: peak, pit, ridge, valley, flat, minimal, saddle ridge, and saddle valley surfaces [12]. Distinguishing all eight surface primitives requires near zero values to be determined for the Gaussian and mean curvatures using thresholds for zero values. Alternatively, concave, convex and saddle regions can be determined without the need for thresholds [5].

3 Mathematical Background

The equations in the next two sections were initially presented in [9]. The basic kinematic equations of motion are provided here as well as the equations for estimating the curvature form of the surface. Section 3.2 describes the equations used to determine the curvature at a point on the fitted a surface.

3.1 Simulating Rolling Motion

The following is the equation for the kinematics of a rigid

probe and rigid object in rolling contact and is based on the gauss maps of both objects. This equation was used to simulate the motion of the rolling fingertip probe on the surface of the unknown object. The contact point on the probe evolves according to the following differential equation of motion:

$$\dot{p}_1 = M_1^{-1}(K_1 + \bar{K}_2)^{-1}\left(\begin{bmatrix} -\omega_y \\ \omega_x \end{bmatrix} - \tilde{K}_2 \begin{bmatrix} \upsilon_x \\ \upsilon_y \end{bmatrix}\right) \qquad (1)$$

Where:

K_1 is the known curvature form of the probe

$\bar{K}_2$ is the curvature form of the object in the probe's contact frame

M_1 is the metric of the probe

$\omega = [\omega_x, \omega_y]$ is the vector containing the angular velocities of the probe's contact frame with respect to the object's contact frame around the x and y axis

υ_x and υ_y are the linear velocities of the probe's contact frame with respect to the object's contact frame in the x and y direction

p_1 is the contact point $[u_1, v_1]$ on the probe

3.2 Curvature Estimation from Rolling Probes

For rolling contact (i.e. no slipping), $\upsilon_x = \upsilon_y = \upsilon_z = 0$ in the above equation of motion. Determining the curvature of the unknown object requires solving the above equation for the unknown curvature form $\bar{K}_2$. Since the inverse of the relative curvature form is symmetric:

$$(K_1 + \bar{K}_2)^{-1} = \begin{bmatrix} k_1 & k_2 \\ k_2 & k_3 \end{bmatrix} \qquad (2)$$

These unknown values can be solved using the equation:

$$\begin{bmatrix} k_1 & k_2 & k_3 \end{bmatrix}^T = (A^T A)^{-1} A^T B \qquad (3)$$

where

$$A = \begin{bmatrix} -\Delta\theta_{y_1} & \Delta\theta_{x_1} & 0 \\ 0 & -\Delta\theta_{y_1} & \Delta\theta_{x_1} \\ \dots & \dots & \dots \\ -\Delta\theta_{y_n} & \Delta\theta_{x_n} & 0 \\ 0 & -\Delta\theta_{y_n} & \Delta\theta_{x_n} \end{bmatrix} \qquad B = \begin{bmatrix} M_1 \Delta p_{1_1} \\ \dots \\ M_1 \Delta p_{1_n} \end{bmatrix}. \qquad (4)$$

The entries $\Delta\theta_{x_n}$ and $\Delta\theta_{y_n}$ are the nth approximation of the sums of the instantaneous rotations about the x-axis and y-axis of the instantaneous contact frames for a particular probe. Once the values of k_1, k_2, and k_3 are solved, equation (2) can be used to solve for $\bar{K}_2$. The diagonal elements of $\bar{K}_2$ are the normal curvatures in the u and v directions.

3.3 Gaussian and Mean Curvature

Consider a surface $Q(u,v)$. The curvature at a point is characterized by the principle curvature directions and the magnitudes of curvature in each direction. If the directional information is not required, the Gaussian and mean curvature can be easily calculated using the following equations. A more complete description can be found in [2], [4], and [5].

Define the variables E, F, G, and e, f, g as:

$$E = \frac{\partial Q}{\partial u} \bullet \frac{\partial Q}{\partial u} \qquad e = \frac{\partial^2 Q}{\partial u^2} \bullet \bar{n}$$

$$F = \frac{\partial Q}{\partial u} \bullet \frac{\partial Q}{\partial v} \qquad f = \frac{\partial^2 Q}{\partial u \partial v} \bullet \bar{n} \qquad (5)$$

$$G = \frac{\partial Q}{\partial v} \bullet \frac{\partial Q}{\partial v} \qquad g = \frac{\partial^2 Q}{\partial v^2} \bullet \bar{n}$$

where $\bar{n}$ is the unit surface normal. The Gaussian and mean curvature are then respectively:

$$Kg = \frac{(eg - f^2)}{(EG - F^2)} \qquad Ka = \frac{(Eg - 2Ff + Ge)}{2(EG - F^2)} \qquad (6)$$

4 Simulation Studies

The first simulation uses the equations of section 3.2 to determine the surface curvature of an unknown object at a point using EP1. Two different test objects are used and the sensitivity of the approach is analyzed.

The second simulation study investigates the ability to extract shape information using EP2.

4.1 Curvature Estimation from Rolling Probes

There are three sources of error in the estimation procedure: measuring the angular velocity, the resolution of the contact sensor, and the length of Δs.

Maintaining rolling contact will require regulating forces in the instantaneous normal and tangent direction to avoid slip while regulating the angular velocity (ω). It cannot be exactly determined how the object's contact frame twists during the course of the rolling probe. It is therefore likely that errors will occur in the measurement of ω as it must be measured instantaneously with respect to the moving contact frame of the object.

The resolution of the contact sensor affects the estimated change in contact position which will also affect calculation of the contact normal and the estimate of the curvature form.

If the point of contact travels far away from the point of interest (long Δs), then the curvature could vary significantly over this interval.

4.1.1 Results for Sphere

The sensitivity of the approach was analyzed by adding noise from a uniform error distribution whose maximum was a specified percentage of the actual angular velocity.

The radius of the probe (R_1) is chosen to be 1 unit. Spheres of radius 500, 50, 5, 1, and 0.5 units (R_2) were probed in simulation to analyze the sensitivity trend. The upper limits for the magnitude for the added noise were: 0.1, 1.0, 5.0, and 10.0% of the magnitude of the angular velocity.

The results in figure 2 show the trend for error due to inaccuracy in ω. The values for ω and the probe duration used for the graph were 0.1 rad/sec and 1 sec respectively. As the RCR decreases the estimated curvature is more sensitive to error in measured angular velocity. It is easy to see from this graph that when the radius of the object is about 50 times that of the probe or higher, the estimate error increases dramatically with measurement error.
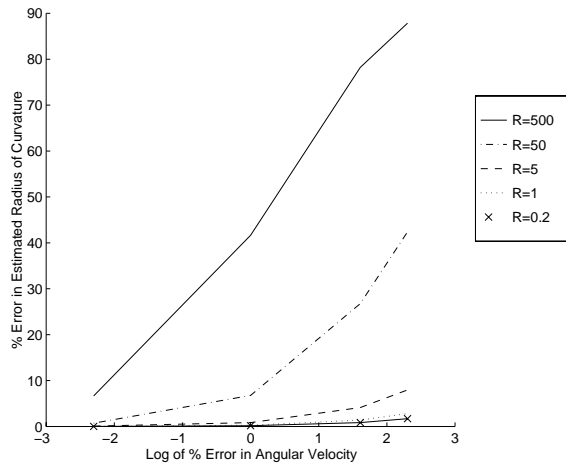

Fig. 2. Effect of Angular Velocity Error

The curvature estimates were not affected by the length of Δs. This was expected for a sphere (or plane) because the constant curvature.

4.1.2 Effects of Changing Δs

Increasing Δs can cause errors in surfaces with non-constant curvature. For this reason a paraboloid of revolution was investigated. The paraboloid was formed by rotating the curve $z = -Cx^2$ about the z axis. Paraboloids with different values for parameter C: 8, 5, 1, 0.5, 0.1, and 0.01 units were probed. These values were chosen because they yield local radii of curvature between 500 and 2.5 units.

The same noise values as the above study were used. It was found that the probing motions had to have a very small Δs to accurately estimate the curvature at the point of interest. The curvature estimate grows rapidly inaccurate as Δs increases. The curvature for the paraboloid could not be accurately estimated for C equal to 5 for a reasonable Δs even without error in ω. The approach is accurate to about 15% error for C values between 1 and 0.01.

4.1.3 Contact Resolution

The above simulations assumed an infinitely accurate con-

tact sensor. This enabled us to determine the error caused by the inaccuracy of ω. The following simulations determine the error caused by the finite resolution of the sensor. The sensor is assumed to be composed of tiny little sensor pads. The sensor pad closest to the point of contact is activated. A probe with a 1 cm radius (R_1) was tested in simulation with the following resolutions: 0.01, 0.1, 0.5, and 1.0 mm. The object being probed was a sphere for the simulation studies in this section.
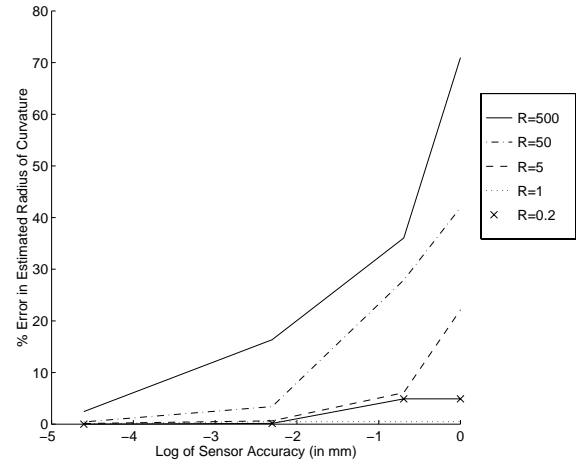

Fig. 3. Effect of Sensor Resolution

The general error trend for the different sensor accuracies is shown in figure 3. The estimation becomes less accurate as the sensor resolution decreases. It was also found that the approach becomes more sensitive to sensor resolution as the RCR decreases. In many of the simulations the estimated curvature was zero for R_2 values above 5 and sensor resolutions coarser than 0.1 mm.

The results for many angular velocities and probing durations were simulated to investigate the combined effect of Δs and the resolution of the sensor. It was found that the accuracy of the estimate improves as Δs increases. However, the object being probed has constant curvature it is not affected by the length of Δs. For objects of non-constant curvature, a satisfactory Δs will have to be determined which improves the estimate but is not overly affected by the changing curvature around the point of interest.

The resolution error would be similar using an insensitive probe and force/moment wrist sensor as in Tsujimura and Yabuta [11]. Using a semi-spherical probe to determine contact position they found their measurement error to vary 2.7 mm on average. From this they determined their tactile sensor system to be accurate to within 2.7 percent of the probe diameter. This would translate to an accuracy of 0.54 mm in our simulation study.

A reasonable estimate for spheres of radius 5 to 0.2 cm can be achieved for an accuracy of 0.5 mm using a rolling duration of 1 second and an angular velocity of about 0.5

rad/sec assuming no errors in ω.

4.1.4 Summary of Results for EP1
Three trends were seen in the simulation studies above:

A) The curvature estimates become less accurate for a given error in the angular velocity measure, and for a given sensor resolution as the RCR decreases.
Equation (1) was simplified by using a sphere of radius R_2 for the object in order to determine the source of the sensitivity to the curvature of the object.

$$
\dot{p}_1 = \begin{bmatrix} \dfrac{1}{\dfrac{R_1}{R_2}+1} & 0 \\ 0 & \dfrac{1}{\left(\dfrac{R_1}{R_2}+1\right)\cos{(u_1)}} \end{bmatrix} \begin{bmatrix} -\omega_y + e_y \\ \omega_x + e_x \end{bmatrix} \quad (7)
$$

It can be seen from the simplified equation (7), as the radius of the second object increases the effect of the errors (e_x and e_y) will also increase.

B) As Δs increases, the accuracy of the estimated curvature decreases for surfaces of non-constant curvature.

C) Δs will have to increase to compensate for the resolution of the sensor in order to get an accurate estimate of the curvature.

The result is that this method will not be able to accurately measure the curvature of planar or near planar surfaces. This is true even for small errors in the measurement of angular velocity, or minute errors in the precision of the sensor. However, the method could be used accurately to verify edges and regions of high curvature.

The error due to sensor resolution is the limiting factor. Given the accuracy of the current sensor technology a relatively long Δs would be required to accurately measure surfaces of moderate curvature which would reduce the accuracy of the curvature estimate.

4.2 Curvature Estimation from a Multifinger Probe
A three fingered probe of the surface is simulated where the hand tracks a 3 x 3 units^2 patch of the surface. The interfinger distance (IFD) is 1 unit and the fingers are constrained to move in parallel planes. Ten points per finger are recorded as the fingers trace over the patch.
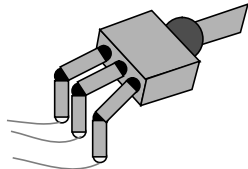

Fig. 4. Three Fingers Tracking a Surface

Several different surfaces were used to test the accuracy of the approximation of Gaussian and mean curvature, and shape. A sphere, cylinder, rotated cylinder, and parabolic saddle were tested. The rotated cylinder was used to test the effect of probing in directions other than along the lines of curvature. Tensor product effects can occur if the surface parameters are not aligned with the lines of curvature [14]. The saddle surface tests the accuracy of curvature based segmentation for a patch composed of several different shape regions.

Our algorithm for fitting the surface is as follows. First, a bi-quadric least squares tensor product surface is fit to the locus of contact points using a smoothing value of s=1000, and a weighting factor of 100 for all points. This acts as a low pass filter for the noise in the position of the contacts. Next, the values of the first surface fit for the initial data points are used for a second surface fit. Surface normal information is incorporated into the surface fitting procedure by inserting points on the tangent line perpendicular to the direction of motion of the hand while probing. The new points are added 0.05 units to each side of the filtered data points on the tangent line. Finally, another smoothing spline is fit using the new set of data points. The FITPACK software package created by Dierckx [3], was used to fit the smoothing spline and calculate the derivative values at points on the B-spline surface.

4.3 Results for EP2
The second iteration of fitting a smoothing spline dramatically increases the accuracy of the estimation. The shape classifications for points on the surface are well estimated for noise values of 5% of the IFD or less. Zero values of the Gaussian curvature were found using a threshold of 0.005 units. Both the Gaussian and mean curvatures were reasonably well estimated. The patches could be further analyzed to determine the directions of principle curvature which could be used to orient the patch.
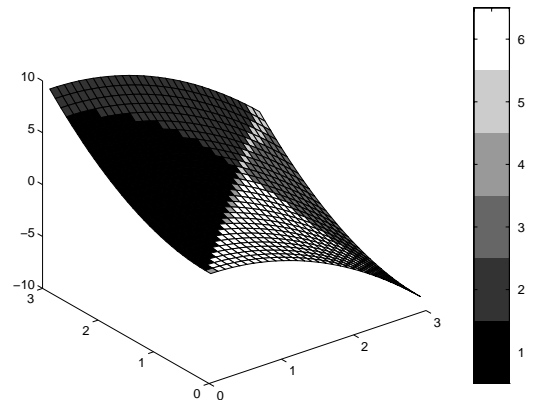

Fig. 5. Saddle Surface Showing Shape Regions

For errors of 10% of the IFD, only the sphere was accurately classified by shape. The mean curvatures were well approximated in the other surfaces, but there was a increase in error for the Gaussian curvatures which caused incorrect classifications of shape.

A segmentation of the saddle surface was performed based

on the eight surface primitives described in section 2.2. The segmentation was mapped onto the fit B-spline surface and is shown in figure 5. A 30 x 30 array of points was evaluated on the surface and the shape primitives calculated. For noise values of 5% of the IFD (as in figure 5) the shape based segmentation had a near perfect correspondence with the actual surface. However, it was found that this type of segmentation is sensitive to errors in the Gaussian curvature which can be incorrectly categorized when the noise level is high.

Some tensor product effects were found while fitting a surface for the cylinders and the saddle using noisy data.

5 Conclusions and Future Work

We investigated the computational feasibility of using Montana's method for EP1 to determine surface curvature. Our investigation of the approach exposed a sensitivity to error in angular velocity, and the resolution of the sensor for surfaces with low curvature.

Regions of high curvature such as edges may be sensed using EP1, however the actual radius may not be measurable given the sensor resolution. This will be the case if the change in the point of contact is less than the sensor resolution for a particular probing motion.

Finite sensor resolution requires a larger region on the surface to be probed which may cause errors in estimation for objects with changing curvature over the probed region.

The method will be unable to accurately estimate surfaces whose curvature is much smaller than the curvature of the probe. The measurement accuracy, resolution of the sensor, and shape of the object will determine the actual upper limit. The best estimates will be for regions where the curvature is close to or greater than that of the probe.

We presented an approach using EP2 to determine the shape properties of an approximating surface from its Gaussian and mean curvatures. The surface patch was approximated by a smoothing spline surface which incorporated the contact normal information. The approach was found to work extremely well for data points with errors of 5% of the IFD or less. The patches could be oriented based on the shape based segmentation of the patch and further analysis of the directions of the principal curvatures.

For errors of 10% of the IFD or more, the method was much less reliable although the mean curvature was still well approximated. More research needs to be done to determine how to better utilize the normal information to improve the shape estimates in the presence of noise.

Since the initial submission of this paper we have developed an elegant method of incorporating surface normals into the surface fitting algorithm [14].

Experiments using a robot and a force/moment wrist sensor will be performed to verify the feasibility of EP1, EP2, and our approach to curvature analysis.

Surface description and recognition from curvature based segmentation will also be investigated in the future. This will include the use of the shape primitives for orienting the patch, and for building higher level shape primitives. The intention is to find better higher level, and qualitative model matching parameters based on the curvature properties of the surface.

6 References

[1] P. K. Allen and P. Michelman, "Acquisition and Interpretation of 3-D Sensor Data from Touch", IEEE T. on Robotics and Automation, Vol. 6, No. 4, pp. 397-404, 1987

[2] R. C. Beach, "An Introduction to the Curves and Surfaces of Computer Aided Design", Van Nostrand Reinhold, New York, 1991

[3] P. Dierckx, "Curve and Surface Fitting with Splines", Clarendon Press, New York, 1993

[4] J. C. Dill, "An application of Color Graphics to the Display of Surface Curvature", Computer Graphics, Vol. 15, No. 3, August 1981

[5] G. Elber and E. Cohen, "Second-Order Surface Analysis Using Hybrid Symbolic and Numeric Operators", ACM Transactions on Graphics, Vol. 12, No. 2, pp. 160-178, April 1993

[6] R. S. Fearing, "Tactile Sensing for Shape Interpretation", Dexterous Robot Hands, S. T. Venkataraman and T. Iberall, Springer-Verlag, 1990

[7] H. Hemami, J. Bay, and R. E. Goddard, "A Conceptual Framework for Tactually Guided Exploration and Shape Perception", IEEE Transactions on Biomed. Eng., Vol. 35, No. 2, pp. 99-109, Feb 1988

[8] S. J. Lederman, R. L. Klatzky and D. T. Pawluk, "Lessons From the Study of Biological Touch for Robotic Haptic Sensing", Advanced Tactile Sensing for Robotics, H. R. Nicholls, World Scientific, 1992

[9] D. Montana, "The Kinematics of Contact and Grasp", The Int'l J. of Robotics Research, Vol. 7, No. 3, pp. 17-31, June 1988

[10] E. Trucco and Robert B. Fisher, "Experiments in Curvature-Based Segmentation of Range Data", IEEE PAMI, Vol. 17, No. 2, pp. 177-182, Feb 1995

[11] T. Tsujimura and T. Yabuta, "Object Detection by Tactile Sensing Method Employing Force/Torque Information", IEEE Transactions on Robotics and Automation, Vol. 5, No. 4, August 1989

[12] N. Yokoya and M. D. Levine, "Range Image Segmentation Based on Differential Geometry: A Hybrid Approach", IEEE Transactions on PAMI, Vol. 11, No. 6, pp. 643-649, June 1989

[13] S. S. Sinha and P. J. Besl, "Principal Patches a Viewpoint Invariant Surface Description", IEEE ICRA, Vol. 1, pp. 226-231, 1990

[14] M. Charlebois, "B-Spline Surface Fitting Incorporating Surface Normal Information", work in progress